Propagating phonons in liquid ^{4}He

1989 J. Phys.: Condens. Matter 1 3507

(http://iopscience.iop.org/0953-8984/1/22/010)

J. Phys.: Condens. Matter **1** (1989) 3507–3522. Printed in the UK

Propagating phonons in liquid ^{4}He

A F G Wyatt†, N A Lockerbie‡ and R A Sherlock§

† Department of Physics, University of Exeter, Stocker Road, Exeter EX4 4QL, UK
‡ Department of Physics, University of Strathclyde, Strathclyde, UK
§ Engineering Development Group, MAF Tech. Ruakura, Private Bag, Hamilton, New Zealand

Received 13 October 1988, in final form 2 December 1988

Abstract. Phonon propagation in liquid ^{4}He at $T \simeq 0.1$ K is studied as a function of pressure input power and propagation distance. Using a superconducting tunnel junction detector it is found that a single injected pulse can form two propagating pulses at low pressures but only one at high pressures. It is shown that three-phonon scattering can explain this behaviour. At low pressures, one group of phonons propagates ballistically while another group consists of strongly interacting phonons which travel at the ultrasonic velocity.

1. Introduction

The propagation of phonons in liquid He at $T = 0$ K is governed to a large extent by the phonon dispersion curve $\omega(q)$ (figure 1) [1]. This is not only because the group velocity $d\omega/dq$ is a function of energy but also because the mean free path against spontaneous decay is qualitatively determined by the subtleties of the shape of $\omega(q)$. Quantitatively, the strength of the decay also depends on the non-linearity of liquid ^{4}He as an acoustic medium.

In this paper, we consider the behaviour of pulses of phonons injected into liquid ^{4}He and their development as they propagate over several millimetres. As liquid He is

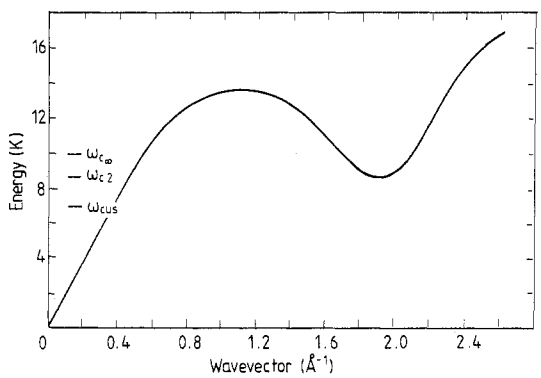

Figure 1. The dispersion curve for liquid ^{4}He at 0 bar [1]. Three cut-off energies are shown as described in § 2.

very compressible, the velocity of phonons varies considerably with pressure. Moreover, the form of the dispersion also varies with pressure and this causes major changes in the propagation characteristics. We shall see that one of the consequences of this is that at low pressures a single pulse breaks up into two groups of phonons travelling at different velocities, while at high pressures it stays as one group.

The phonon dispersion curve of liquid ^{4}He has been of interest since the T^3 specific heat led to the suggestion of a linear phonon form for $\omega(q)$ [2]. For many years it was thought that $\omega(q)$ departed from linearity, as q increased, by bending downwards. At high phonon energies there is always a downward trend which eventually leads to the maxon peak, which at 0 bar is at $\omega = 14$ K ($\hbar\omega = kT$ is implied throughout) and $q = 1.1$ Å^{-1}. The neutron scattering data seemed to support this view. However, the ultrasonic attenuation calculated with this assumption could not account for the large measured values and it was pointed out that upward bending of $\omega(q)$ could reconcile matters [3]. This initial upward bending of $\omega(q)$ is called anomalous dispersion.

The most important consequence of upward curvature of $\omega(q)$ is that it allows spontaneous decay of a high-energy phonon into two smaller phonons. This three-phonon process is forbidden if the curvature is downwards because energy and momentum cannot be conserved. In this case the only scattering is from thermal phonons, by four-phonon processes [4]. This is a much weaker process which can be made negligibly small by going to low enough temperatures.

The upward curvature is small and it is difficult to detect by ultrasonic velocity or specific heat measurements. Clear evidence comes from the spontaneous decay of high-energy phonons. When a single phonon spontaneously decays into two phonons, the requirement for energy and momentum conservation means that the propagation directions of the two decay phonons are angularly separated. The angular spreading of a phonon beam enables this angle to be detected [5]. The decay angle decreases to zero at a pressure of 19 bar, showing that at this pressure the anomalous dispersion changes to normal dispersion which then increases with pressure.

At pressures where there is anomalous dispersion, the upward curvature of $\omega(q)$ at low q must change to downward curvature at high q. The phonon energy at which this happens we loosely call the critical energy ω_c. There are in fact several critical points which we shall consider more carefully below. The pressure dependence of the ultrasonic attenuation led to the idea that ω_c is a function of pressure and decreases with increasing pressure [6].

Such critical energy implies that phonons injected into liquid He with $\omega < \omega_c$ have a short mean free path because they decay rapidly into low-energy phonons, whereas injected phonons with $\omega > \omega_c$ have longer mean free paths as this spontaneous decay process is not available to them. This idea was tested by using superconducting tunnel junctions in two different experiments [7, 8]. These experiments show that high-energy phonons do have a long mean free path and that ω_c decreases with increasing pressure. Measurements at different distances shows that the high-energy phonons with $\omega > \omega_c$ have mean free paths greater than 10 mm.

Since these measurements there have been improvements in the neutron determination of $\omega(q)$ and the upward dispersion has been measured in some detail at 0 bar [9]. Also high-energy phonons have been used in quantum evaporation experiments and it is clear that phonons with $\omega \simeq 11$ K can propagate without scattering [10].

In this paper, we examine the consequences of the critical energy on an injected spectrum of phonons. We shall see that phonons with $\omega > \omega_c$ propagate ballistically and without interaction if the liquid ^{4}He temperature is low enough. Phonons injected with

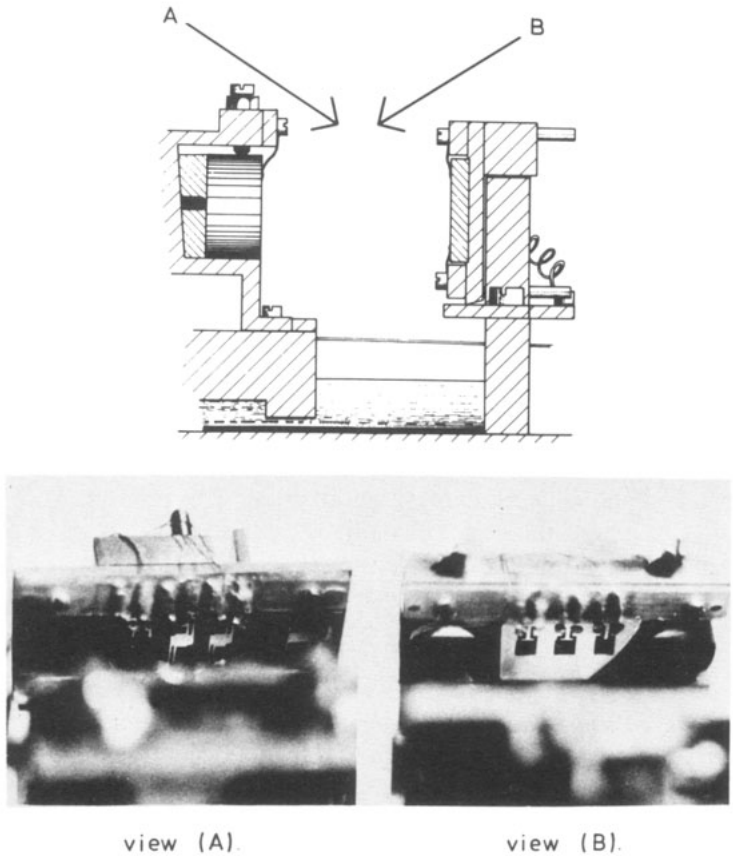

Figure 2. Diagram of the apparatus shows the carriage on the left-hand side resting on the cylincrical track and holding the large sapphire crystal. Opposite it is the fixed holder of the detector substrate. The photograph taken from view A shows two tunnel junctions (centre and right) and a graphite bolometer. View B shows three thin-film heaters on the asymmetric face of the sapphire crystal.

$\omega < \omega_c$ decay rapidly and form an interacting group. The two groups can be distinguished by time-of-flight measurements with a superconducting tunnel junction detector.

2. The physical system

Phonons with a wide spectrum of energies can be injected into liquid ^4He, in a short (about 1 μs) burst from a pulse heated metal film. After propagating some millimetres through the liquid ^4He, they are detected by a superconducting tunnel junction. The arrangement is shown in figure 2 and is described in § 3. If the ^4He is sufficiently cold, $T \leqslant 0.05$ K, then the thermal ambient excitations can be neglected and the propagation of injected phonons depends on the intrinsic acoustic properties of the liquid ^4He. In the simplest case an injected phonon might propagate ballistically without interaction. On the contrary, the injected phonons can decay and also strongly interact with other injected phonons. It is the purpose of this paper to establish in broad terms what happens

to an injected spectrum of phonons. We shall see that it depends both on the intensity of the injected phonons and on the pressure of the liquid ^{4}He.

The experiments necessarily involve the injection and detection of phonons as well as their propagation in the liquid ^{4}He. We must first discuss what is injected and detected before we can interpret the signals to discover what happens during the propagation.

Phonons in these experiments are injected essentially from a heated thin metal film. The heating pulse is long (1 μs) compared with the thermal time constant of the film (about 30 ns) and so there is a dynamic equilibrium between the electrical heat input and the phonon (and roton)† output. So, during the pulse, essentially the same energy spectrum of phonons is continuously injected. The injected spectrum has been measured in various ways. It is important to remember that the injected spectrum of phonons is certainly not the same as the phonon spectrum inside the thin metal film. This is because there are strong processes at the interface between the film and the liquid ^{4}He that down convert the phonon energies [11–13]. It appears that a phonon in the metal film usually creates two or three phonons in the liquid ^{4}He and there is only a low probability of creating a single phonon with energy conservation. This interface scattering not only reduces the energies of the injected phonons but also prevents the injected phonons from being emitted into a narrow cone, about the interface normal, which otherwise would be expected from the conservation of parallel momentum at the interface.

One measurement of the injected spectrum uses the velocity dispersion at 24 bar which can be calculated from $\omega(q)$ measured by neutron scattering [14]. This method is sensitive to the higher-energy part of the spectrum as the low-energy phonons show little dispersion. If the spectrum is taken to be a Planck distribution, the characteristic temperature is found to be about 0.7 K and is relatively insensitive to input power over a considerble range. However, this technique is insensitive to the small number (less than 1%) of very-high-energy phonons with $\omega > 10$ K.

Another measurement uses the pressure dependence of a signal detected by a superconducting tunnel junction [8]. At low injected powers, the only phonons which are detected are those with $\omega > \omega_c$. If ω_c is then varied by pressurising the liquid ^{4}He, the high-frequency tail of the phonon spectrum can be found. The exponential increase in signal with pressure is consistent with the high-energy tail of a Planck spectrum, i.e. $\omega^2[\exp(\hbar\omega/kT) - 1]^{-1}$. The characteristic temperature found by this method is about 1 K with $\omega_c = 10$ K, which is not significantly different from 0.7 K found by the dispersion measurement. In fact the agreement is very good considering the independence of the two methods. We shall take the injected phonons to have mainly a Planck spectrum with a characteristic temperature of 0.9 K, and the effect of pulse power is to change the intensity of the spectrum by the same factor at all energies. There will also be a small fraction of phonons emitted with a characteristic temperature that is the same as the heater temperature.

In the present measurements the detector is an Al/I/Al superconducting tunnel junction. Only phonons large enough to break Cooper pairs give a signal; so the detector is only sensitive to phonons with $\hbar\omega > 2\Delta_{Al}$, i.e. 4.2 K. A phonon incident on the detector has a probability of less than unity of being absorbed. For high-energy phonons this probability is relatively high and the meagre evidence suggests that it is energy independent for $\omega > 5$ K [16]. Although we shall assume this, it is not critical for the

†Although rotons are certainly injected into the liquid ^{4}He, they are not detected and for the purposes of this paper can be neglected. Rotons probably do have the effect of shortening the injected phonon pulse by scattering the phonons injected later in the pulse. The effective phonon pulse length is probably 0.2→0.3 μs [15] for high energy phonons.

interpretation of the measurements. The quality of the superconducting tunnel junction is particularly good and there is little sign that it detects a measurable signal from phonons with $\hbar\omega < 2\Delta_{Al}$.

As mentioned earlier, the effect of upward curvature of the dispersion curve is to allow spontaneous decay. There are various critical energies [17] and, in order of increasing energy, they are as follows.

(1) The three-phonon ultrasonic cut-off is the highest-energy phonon that can absorb or emit an ultrasonic phonon, i.e. a phonon with $\omega \rightarrow 0$ which travels at the ultrasonic velocity. The criterion is the equality of the group velocity of the high-energy phonon and the ultrasonic velocity. For 0 bar, $\omega_{c,us} = 7.0 \pm 0.6$ K from neutron data [9].

(2) The three-phonon high-energy cut-off is the highest energy at which a phonon can decay into two phonons. This occurs when the two phonons have equal energies and so the criterion is the equality of the two phase velocities: $v_p(\omega_{c2}) = v_p(\omega_{c2}/2)$. From the neutron data, $\omega_{c2} = 8.6 \pm 0.2$ K.

(3) Above this energy a phonon can only decay into three or more phonons. The limit is when an infinite number of ultrasonic phonons are produced. The criterion for this is when the phase velocity of the high-energy phonon equals the ultrasonic velocity. From neutron data, we find that $\omega_{c\infty} = 10.0 \pm 0.1$ K.

These critical energies are shown in figure 1 for 0 bar.

The strength of the three-phonon decay has been calculated [17, 18]. The mean free path varies as ω^5 for $\omega < \omega_{c2}$. The mean free path is less than 2 mm, which is the smallest distance used in our experiment, for phonons with $\omega > 0.7$ K. At $\omega \simeq \omega_{c2}$ the mean free path is very short, about 10^{-8} m. The higher-order decays are likely to be weaker, but there are no measurements of mean free paths with which to compare these estimates. However, it is clear that there is a dramatic difference in mean free path at $\omega \simeq 10$ K and that above this energy the mean free path is many millimetres [10]. The fact that the measured value for energy cut-off 9.5 ± 0.5 K [7] at 0 bar compares with $\omega_{c\infty} = 10.0 \pm 0.1$ K estimated from the neutron data suggests that only phonons with $\omega > \omega_{c\infty}$ have macroscopically long mean free paths. However, as this identification is not necessary for the subsequent discussion, we shall use ω_c to indicate the lowest energy for macroscopic mean free paths.

In figure 3(*a*) is shown the best estimate for the spectrum of injected phonons. It consists of two Planck spectra: one for the phonons that are down converted at the heater–^{4}He interface (background phonons) with a temperature of 0.9 K, and the other for the elastically transmitted phonons (peak phonons) with a temperature of 1.85 K. This is the temperature of the heater for a −20 dB (reference 0.5 W mm^{-2}) input pulse [19]. The ratio of peak to background phonons is 5×10^{-3} and is chosen so that the contributions from the Planck spectra are equal at $\omega = 10$ K, so that for $\omega < 10$ K the spectrum is dominated by the 0.9 K Planck spectrum and for $\omega > 10$ K it is dominated by the 1.85 K spectrum. This is consistent with the experiments described earlier which are sensitive to $\omega < 10$ K phonons.

The only measurements of the peak-to-background ratio are with single crystals. For NaF it is 5×10^{-2} [20], which is an order of magnitude larger than that taken for the metal film heater. As the peak channel for phonon transmission decreases as the interface becomes less ideal, then this difference is reasonable. We expect the peak phonons to have a wider angular distribution from the metal film than from the cleaved NaF surface owing to the roughness of the evaporated film. We in fact assume that the peak and background angular distribution are the same for the metal film. The two Planck spectra

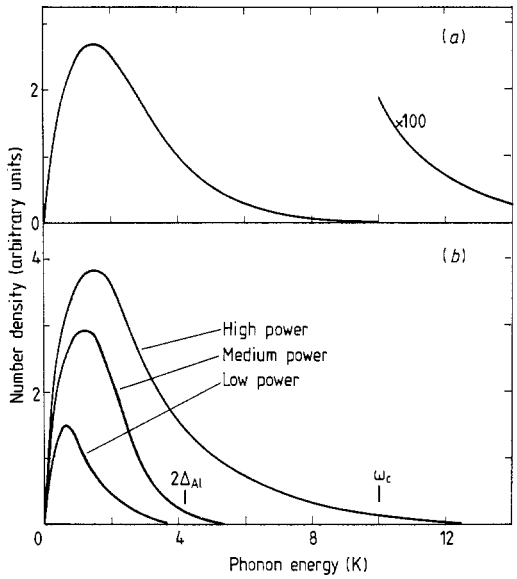

Figure 3. (*a*) The calculated phonon number density as a function of phonon energy. It is the sum of two Planck spectra: one at 0.9 K and the other at 1.85 K. This corresponds to a −20 dB (reference 0.5 W mm^{-2}) input pulse. (*b*) Schematic phonon number densities that occur after propagation through the liquid ^{4}He. The three curves correspond to low, medium and high injected input powers.

give a very good fit to the superconducting tunnel junction signal as a function of pressure, and this will be discussed in a later publication.

From figure 3(*a*) it can be seen that the number of phonons with $\omega > 10$ K is of the order of 1% of the total number. In figure 3(*b*) are shown schematically the phonon spectra that develop after propagation through the liquid ^{4}He at low pressures. The three curves are for low, medium and high heater powers. The change in the spectra from that in figure 3(*a*) arises from three-phonon processes. At low injected powers the spectrum is due to the decay of injected phonons. The result is a concentration of phonons at low ω. For medium injected powers the density of phonons is high enough for there to be energy up-scattering by three-phonon processes [21] as well as decay. This pushes the spectrum to higher ω. For high injected powers the spectrum is pushed even higher.

For medium and high injected powers, we expect an interacting group of phonons to be produced with a dynamic balance between up- and down-scattering. In the three-phonon processes at low ω, the scattering is approximately collinear, which enables an equilibrium to be attained with much lower phonon densities than those in isotropic thermal equilibrium. The phonons injected with $\omega > \omega_c$ do not scatter by the three-phonon processes and so they will propagate ballistically.

Along the energy axis of figure 3(*b*) is shown the energies of $2\Delta_{Al}$ and ω_c. As the superconducting tunnel junction (STJ) is only sensitive to phonons with $\omega > 2\Delta_{Al}$ it can be seen that, at low injected powers, only phonons with $\omega > \omega_c$ are detected. For medium powers there are two groups of phonons, one with $\omega \geqslant 2\Delta_{Al}$ together with the $\omega > \omega_c$ phonons. At high powers the large number of interacting phonons at high energies means that only phonons with $\omega \geqslant 2\Delta_{Al}$ will be seen.

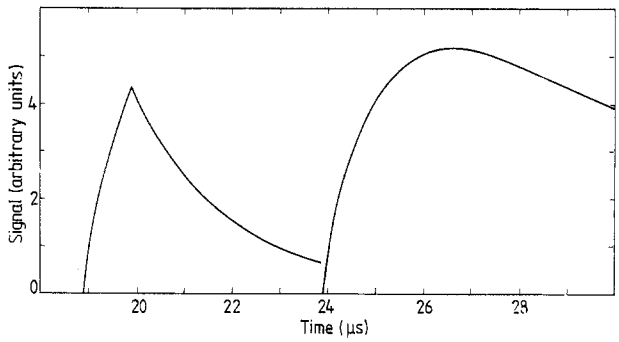

Figure 4. The calculated phonon signal at a bolometer 4.8 mm from the heater for a ^4He pressure of 0 bar. The faster signal is from the interacting phonon and the slower one from the $\omega > \omega_c$ phonons for the distrbution shown in figure 3(*a*). The detector time constant is 2 μs. The relative heights of the two signals are arbitrary.

The two groups of phonons produced at medium powers propagate through the liquid He in different ways. To compare with experiment, we must calculate the time-dependent flux at the detector. For phonons with $\omega > \omega_c$ which propagate ballistically, the flux is given by the dispersion curve. For a delta function input of phonons with spectrum $N(\omega)$ the flux at time t is given by

$$\Phi \propto N(\omega) v_g^2 (\mathrm{d}v_g/\mathrm{d}\omega)^{-1} \tag{1}$$

$$t = l/v_g \tag{2}$$

where $v_g = \mathrm{d}\omega/\mathrm{d}q$, the group velocity, is a function of energy ω and l is the propagation distance. The detected signal also depends on the length of the injected pulse and the time constant of the detector. For the experiment these are about 0.3 and about 2 μs, respectively. In figure 4 is shown the computed signal as a function of time. The $\omega > \omega_c$ phonons form the slower of the two pulses shown.

The integrating group of phonons travel to a good approximation at the ultrasonic velocity v_{us} as long as the tail does not extend too high in ω. Although phonons with $\omega = 2\Delta_{Al}$ travel more quickly than v_{us}, in the interacting group most of the time is spent at energies $\omega < 2\Delta_{Al}$ and relatively little time at $\omega \geqslant 2\Delta$. So, although a phonon must have $\omega \geqslant 2\Delta_{Al}$ at the detector to make a signal, it is created from two slower low-energy phonons. The input of low-energy phonons is not so affected by roton scattering and so the full pulse length of 1 μs is taken. The interacting phonons give the faster of the two pulses shown in figure 4.

For high injected powers, the interacting group of phonons will be dense and their spectrum will extend over all energies. This will give rise to a large and dispersed signal and the non-interacting phonons with $\omega > \omega_c$ will be negligible in comparison.

From these considerations it is expected that there will be three different types of signal as the input power is varied. At high powers there will be a large signal rising rapidly at $t = l/v_{us}$ and extending over long times owing to the population of the slow high-energy modes. At medium powers there should be two signals: a short fast one at $t = l/v_{us}$ from the interacting phonons and a slower dispersed pulse starting at $t = l/v_g(\omega_c)$ from the non-interacting ballistic phonons with $\omega > \omega_c$. At low powers the interaction signal should be absent but there should be a weak signal from $\omega > \omega_c$ ballistic phonons.

3. Experimental arrangement

The experimental cell of liquid ^{4}He is cooled to $T < 0.1$ K by a dilution refrigerator. Inside the cell there is a carriage running on a track which is moved by a stepper motor with superconducting windings (see figure 2). The thin-film heater is mounted on the carriage and the detector is on a bracket at one end of the track. The separation between the heater and detector is variable from 2.2 to 11 mm. The kinematic design ensures that the heater and detector substrates remains parallel. The separation of the heater and detector is found from the time of flight of the ultrasonic phonons.

The STJ is made on a 1 mm-thick sapphire substrate by first evaporating 1500 Å of Al which is then exposed to air at atmospheric pressure for about 4 min to form the oxide tunnel barrier. The junction is completed with another 1500 Å of Al. The energy gap from the I–V characteristic is 0.365 meV, which is equivalent to 4.2 K. The substrate for the heaters is a single crystal of sapphire which extends about 12 mm back from the front face. This prevents any spurious effects from phonons being trapped in the substrate–film interface. Also on the sapphire substrate is another heater facing a colloidal graphite DAG detector. The heater dimensions are 1 mm × 1 mm.

Particular care is taken to avoid loops in the electrical connections to the heater and detector. This minimises the electrical cross talk and allows signals to be measured soon after the input pulse. This is important at short distances where, if the cross talk is large, the recovery of the amplifier can distort the baseline.

The superconducting tunnel junction is in a small magnetic field in order to suppress Josephson currents. The signal from the STJ is amplified and captured on a transient recorder (Biomation 8100). As the signals are very small compared with the noise, many repetitions are averaged, on a Nicolet 1072. For the weakest signals at 0 bar, over 10^5 transients are averaged.

4. Results and discussion

Measurements are made at various input powers, distances and pressure. To see the two signal pulses that were predicted in § 2, there are optimum combinations of these parameters. So, although they cannot be treated completely separately from each other, we shall for clarity consider them in turn.

4.1. Power dependence

In figure 5 is shown a typical power dependence for low pressures and middle to large distances. At high input powers (−11 dB or more) (reference 0.5 W mm^{-2}) there is a large signal which is very dispersed in time. At −14 dB there are clearly two signal pulses: a fast narrow one and a dispersed slower one. At −17 dB the two signals are again clearly evident; however, although the first pulse has decreased, the second is larger than at −14 dB. Except for this last effect the behaviour is as predicted in § 2.

In figure 6 is shown the height of the interacting signal as a function of input power at 0 bar. The very rapid increase in signal with increasing power supports the attribution of this signal to the interacting phonons. A non-interacting group of phonons would only increase linearly with increasing power under the condition that the characteristic temperature did not change with power, whereas the production of relatively high-

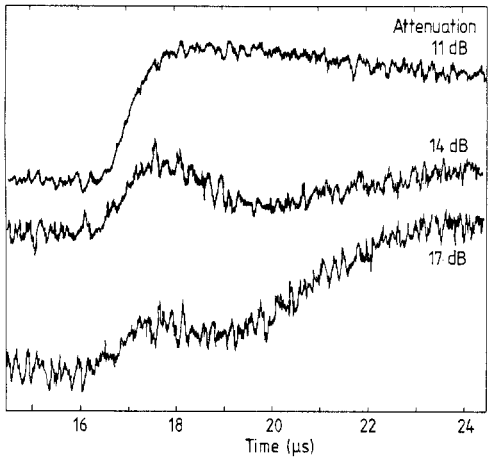

Figure 5. Measured signals at three different input powers, for a heater-to-detector distance of 4.5 mm and a ^{4}He pressure of 4.1 bar. At the two lower powers the interacting phonon pulse can be distinguished from the $\omega > \omega_c$ phonon signal. To obtain relative signal sizes the 11 dB trace should be multiplied by 2.

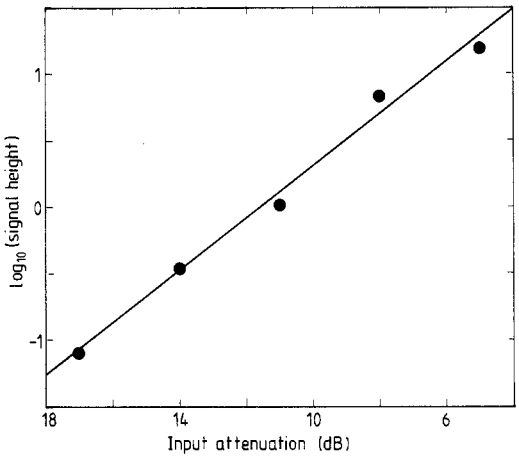

Figure 6. The height of the interacting phonon signal at $t \simeq l/v_{us}$ is shown as a function of input power. The full line has a gradient of 2.

energy phonons with $\omega \geqslant 4.2$ K ($2\Delta_{Al}$) from interactions between low-energy phonons, $\omega < 1$ K, is expected to rise more rapidly than linearly.

The decrease in the $\omega > \omega_c$ signal as the power is increased, shown in figure 5, suggests that this slower signal is attenuated at higher powers by the dense group of interacting phonons. The slow $\omega > \omega_c$ ballistic phonons are injected for approximately the first 0.3 μs of the 1 μs heater pulse and they will be overtaken by the large cloud of interacting phonons emitted after the high-energy phonons. Hence the high-energy phonons can be scattered by four-phonon processes. This is similar to the scattering of high-energy phonons by thermal phonons which has been shown to be a significant attenuation process [22].

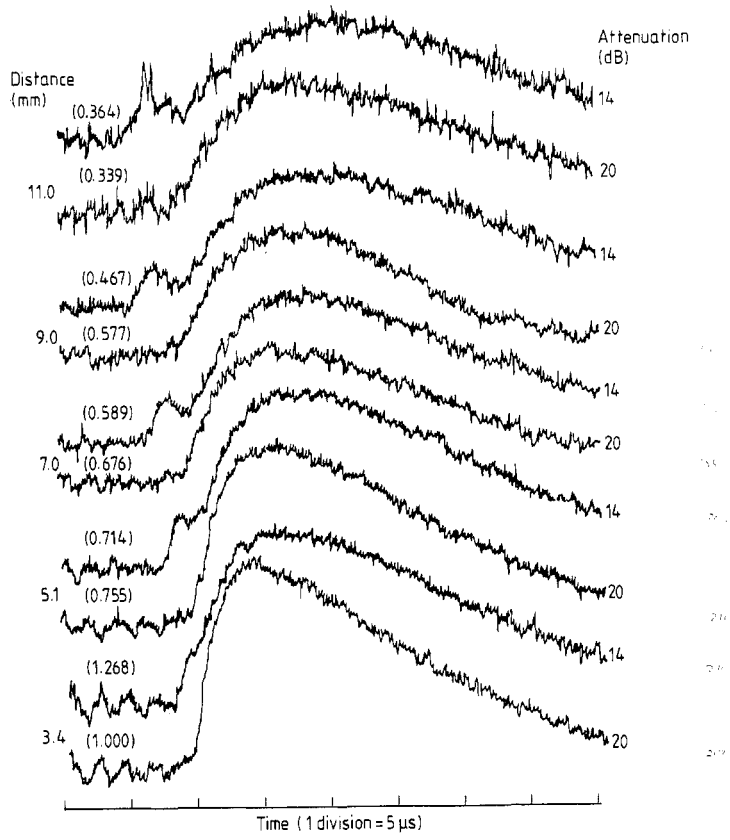

Figure 7. Measured signals at two powers for several propagation distances are shown for a He pressure of 6 bar. The two traces for each distance have the same time scale. For different distances the pairs are offset along the time axis so that the start of the $\omega > \omega_c$ signals are coincident. To obtain relative signal sizes, the traces shown should be multiplied by the scale factors shown in parentheses.

Similar behaviour to that shown in figure 5 can be seen at all pressures between 0 and 8 bar. At lower pressures the time separation of the two-phonon groups is larger but the signals are smaller.

4.2. Distance dependence

In figure 7 are shown the detected signals at different distances at two powers, −14 dB and −20 dB, respectively, at a pressure of 6 bar. The starts of the $\omega > \omega_c$ signals are aligned vertically in the figure and the two traces in each pair have the same time scale. It can be seen that the interaction pulse which is clearly evident at −14 dB is absent at −20 dB. However, the $\omega > \omega_c$ phonons are present at both powers. The effect of velocity dispersions with distance can be clearly seen.

The behaviour at zero pressure has a special importance in view of the many experiments done on liquid ^{4}He at the saturated vapour pressure. Measurements that require a free surface can of course only be done at essentially zero pressure. At this pressure the cut-off phonon energy ω_c is highest and so the number of phonons above ω_c is much

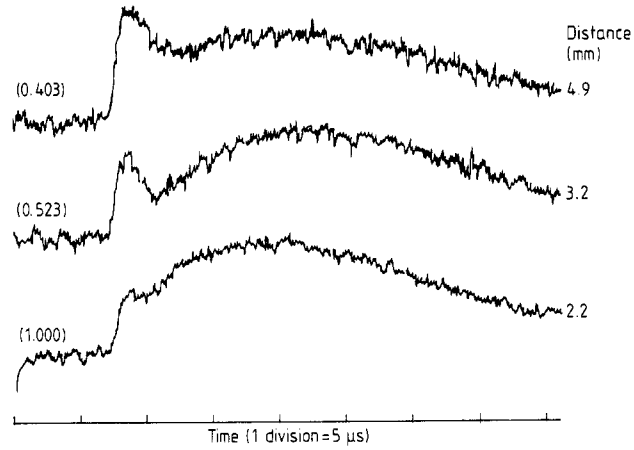

Figure 8. Measured signals at 0 bar and 14 dB attenuation are shown at three distances. Each curve is offset along the time axis so that the start of the interacting phonon signal are coincident. To obtain relative signal sizes, the traces shown should be multiplied by the scale factors shown in parentheses.

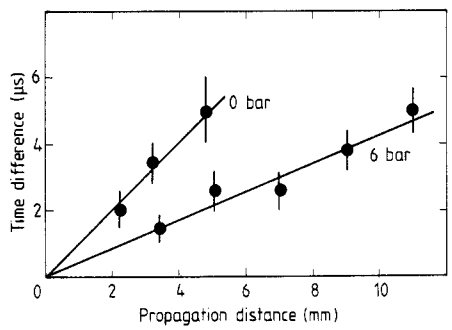

Figure 9. The time difference between the start of the interacting and $\omega > \omega_c$ phonon pulses in figures 5 and 6 are shown as a function of distance. It is clear that the pulses separate linearly with distance.

smaller owing to the exponential tail of the energy spectrum. The signal-to-noise problem is most extreme at this pressure; however, the difference in velocity between phonons with energy $2\Delta_{Al}$ and ω_c is expected to be largest.

In figure 8 is shown the measured signals at three distances at 0 bar. In general behaviour these are similar to those found at other pressures $\leqslant 8$ bar. The two components in the signal are clear, even at the smallest distance, which directly shows that the velocity difference is greatest at 0 bar because ω_c has its maximum value here.

The separation Δt in time of any two similar points on the signal which arise from different velocities v_1 and v_2 is given by $\Delta t = l(1/v_1 - 1/v_2)$. So for the same features at different distances we expect $\Delta t \propto l$. In figure 9 is shown the time differences between the start of the fast and slow signals plotted against the heater–detector separation. The linear dependence on distance can be seen at both 0 and 6 bar. This supports the propagation picture that we have described.

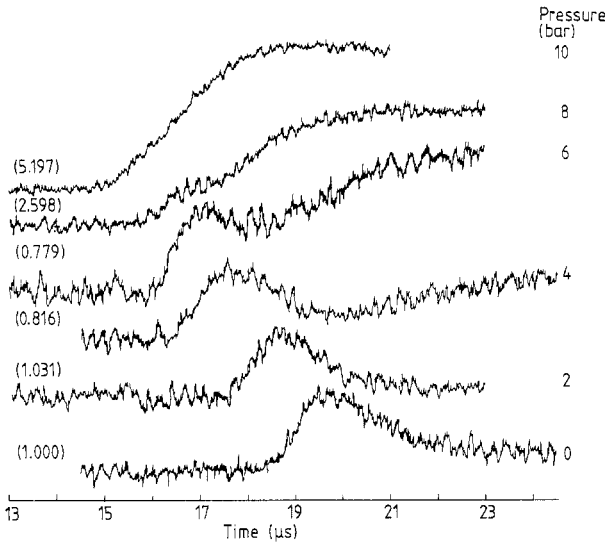

Figure 10. Measured signals are shown for different liquid ^{4}He pressures for a propagation distance of 4.6 mm. The time is measured from the start of the input pulse (14 dB attenuation). The time difference between the start of the interacting and $\omega > \omega_c$ phonon signals can be seen to decrease with increasing pressure. The $\omega > \omega_c$ phonon signal increases with increasing pressure owing to the reduction in ω_c. To obtain relative signal sizes, the traces should be multiplied by the scale factors shown in parentheses.

4.3. Pressure dependence

As the ^{4}He pressure is increased from 0 bar, the phonon cut-off energy decreases and so moves to a straighter part of the dispersion curve. Also, as the pressure is increased, the initial part of the dispersion curve straightens out. The combination of these two effects means that the velocity difference between the ultrasonic value and $v_g(\omega_c(P))$ becomes very small for pressures $P \gtrsim 10$ bar.

The two components of the signal, which are clearly seen at lower pressures, cannot be resolved above 8 bar. This can be seen in figure 10. However, it is still possible to measure the effect of the small difference between v_{us} and $v_g(\omega_c)$. This is done by comparing signals at high and low input powers. At high powers the signal is dominated by the interacting phonons and so the fastest component has velocity v_{us}. At low enough powers the interaction signal becomes insignificant and the received signal only shows the phonons with $\omega = \omega_c$. As $\omega_c(P)$ is lower, the signals are larger and so it is possible to obtain a good signal-to-noise ratio even at low powers at these pressures.

To obtain Δt from such signals, it is necessary to adopt a consistent procedure that circumvents the problem of trying to decide where the signal emerges from the noise. The procedure used here is simply to draw two straight lines: one through the noisy baseline and the other through the linearly rising part of the signal and take the time at the point of intersection. At the lower pressures where the two components are resolved, a similar procedure is used at the beginning of the first and second pulses. The errors are relatively large at the lowest pressures owing to the weak signals.

In figure 11, Δt is shown as a function of pressure. Data from different distances are linearly scaled to the arbitrary distance of 4.8 mm. It can be seen that Δt decreases much more rapidly with increasing pressure at low pressure than at high pressures.

The dispersion curve determined by neutron scattering at 0 bar can be used to calculate Δt. As $\Delta t = l[v_{us}^{-1} - v_g(\omega_c)^{-1}]$ we need $v_g(\omega_c)$ from $\omega(q)$. Neutron measure-

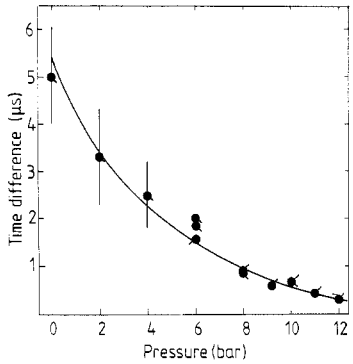

Figure 11. The time difference between the start of the interacting and $\omega > \omega_c$ phonon signals is shown as a function of pressure. The data for 4.8 mm (●) are shown in figure 8. Other data (◐, 11.3 mm; ◑, 9.5 mm) are linearly scaled to a distance of 4.8 mm. The full line is calculated as described in the text.

ments give ω and q pairs; so the phase velocity $v_p = \omega/q$ can be found as a function of q. It is then useful to use the relationship

$$v_g(\omega) = v_p(\omega) + q(\mathrm{d}v_p/\mathrm{d}q)|_\omega. \tag{3}$$

From $v_p(q)$, we find $\omega_{c\infty} = 10.0$ K and, from equation (3), we get $v_g(\omega_{c\infty}) = 187$ m s^{-1}. Using the ultrasonic $v_{us} = 238$ m s^{-1}, we find for $l = 4.8$ mm that $\Delta t = 5.5$ μs. This agrees very well with the measured value of 5.0 ± 1 μs.

The neutron data at other pressures are not good enough to estimate either $\omega_{c\infty}$ or $\mathrm{d}v_p/\mathrm{d}q$. We estimate $v_g(\omega_{c\infty})$ in the following way. We cannot know whether the measured value of $\omega_c(P)$ [6] is $\omega_{c\infty}$ or some other cut-off, but it is the relevant energy for this calculation. However, we do use the relation $\omega_c = v_{us}q_c$ to find q_c. This is only strictly correct for $\omega_{c\infty}$ but at most makes a few per cent difference to q_c at low pressures and less at high pressures. It is more difficult to say how $\mathrm{d}v_p/\mathrm{d}q|_{\omega_c}$ varies with pressure and, in the absence of anything better, we linearly extrapolate from the value of -92.5×10^{-10} m^2 s^{-1} at 0 bar to zero at 19 bar where there is no upward dispersion. Again taking $v_p(\omega_c) = v_{us}$, we calculate Δt. The results are shown in figure 9 as the full line. We see that the calculated Δt shows the same dependence on pressure as the measured data and in fact there is good quantitative agreement over the whole range. The values used in the calculation are tabulated in table 1.

5. Further discussion

The results presented in § 4 strongly support the model outlined in § 2. A high-power heater pulse injects a high density of phonons (and rotons) which, with normal (downward) dispersion, propagate ballistically and the high-energy phonons cause the pulse to disperse. At low pressures, where there is initial upward dispersion, the phonons with

Table 1. Values used in the calculation of Δt.

Pressure (bar)	ω_c (K)	q_c (Å^{-1})	$-dv_p/dq$ (10^{-10}m^{2}s^{-1})	v_{us} (m s^{-1})	$v_g(\omega_c)$ (m s^{-1})
0	10.0	0.550	92.5	238	187
2	9.25	0.477	82.2	254	215
4	8.38	0.411	72.6	267	237
6	7.62	0.359	63.0	278	255
8	6.70	0.303	53.1	289	273
10	5.72	0.250	43.6	299	288
12	4.70	0.199	34.0	309	302
14	3.60	0.147	24.1	320	316

$\omega < \omega_c$ strongly interact with both down- and up-energy conversion. As the scattering angles are not very large, the pulse disperses in time mainly through the velocity spectrum rather than by extra path length. In fact the signals at -10 dB are similar at all pressures, which indicates a substantial population of the high-ω modes from either injection or scattering or from both. At medium powers (-14 dB) the signal at high pressures (about 15 bar or more) is less dispersed than at high powers, owing to the smaller occupation of the high-energy phonon modes.

At low pressures (about 8 bar or less) there are two components to the signal. The faster one is the remnants of the interacting phonons which at medium powers only involve energies up to about 2Δ and so is not dispersed to any significant extent. This pulse travels at the ultrasonic velocity, or perhaps marginally above it, because phonons spend most of their time at low energies. A signal is caused by phonons created with $\omega > 2\Delta_{Al}$ near to the detector, so that they can reach it without decay. The slower signal at medium powers is due to phonons injected into the liquid ^{4}He with $\omega > \omega_c$, where ω_c is probably $\omega_{c\infty}$. These phonons are small in number and are highly dispersed. The fastest phonons in this group travel at $v_g(\omega_c)$.

At low powers (-20 dB) and high pressures the signal shows little dispersion as mainly low-energy phonons are injected. At low powers and pressures, only the phonons with $\omega > \omega_c$ give a signal, as the interacting phonons have such a low density that the up-scattering to $\omega > 2\Delta_{Al}$ is negligible. The $\omega > \omega_c$ phonons are considerably dispersed. This signal hardly falls off with power in the range from -14 to -17 dB. This is probably because the $\omega > \omega_c$ phonons are scattered by the interacting phonons at about -17 dB or less. As the power is reduced, the decrease in this scattering compensates for the lower injected phonon flux.

The strong power dependence of the first pulse supports the picture that it is due to interacting phonons. As a first approximation it is reasonable to assume that the probability of up-scattering to an energy $\omega \simeq 2\Delta_{Al}$ depends on the square of the number density of phonons formed by decay. This density is proportional to the injected power as nearly all the injected phonons have $\omega < \omega_c$ at low pressures. We should then expect the signal from the interacting pulse to vary with the square of the input power, as indeed it does over a limited range of powers.

As this power dependence persists at low powers, it suggests that the superconducting tunnel junction is very nearly ideal and generally detects a usually negligibly small fraction of the low-energy phonons with $\omega < 2\Delta_{Al}$. Also the fact that at low enough powers, at low pressures, the fast signal disappears while the $\omega > \omega_c$ signal is still evident

indicates that any non-ideal detection is small, as the $\omega > \omega_c$ flux is less than 1% of the total.

Measurements of the velocity, over a fixed distance, of the fastest signals at high powers show that it is the same as the ultrasonic velocity for pressures of about 13 bar within the ±1% experimental error. Now the upward dispersion at 0 bar as measured by neutron scattering indicates a group velocity of 262 m s^{-1}, for $\omega = 2\Delta_{Al}$. This is measurably faster than the ultrasonic velocity and it is clear that this is not observed. Phonons of this velocity are injected but they decay before reaching the tunnel junction. The fact that the interacting phonons travel on average at the ultrasonic velocity implies that most of the time is spent at low-energy phonons.

The identification of the second pulse with high-energy phonons that travel ballistically from the heater to the detector is supported by a variety of evidence. This signal increases approximately exponentially with increasing pressure as is expected from the combination of a Planck distribution and ω_c varying linearly with pressure. Also phonons of these energies (about 10 K or more) are seen in quantum evaporation experiments [9] and the fastest phonons in this group travel with the expected velocity of $v_g(\omega_c)$.

The second pulse shows considerable dispersion, which is to be expected if it is due to a spectrum of high-energy ballistic phonons. However, the shape of the pulse is not quite as we predicted in figure 4. This shape essentially comes from a sharp change in the mean free path at ω_c, the exponentially decreasing spectrum and the detector time constant. The measured pulse shapes do not show such a rapid rise but rather show a more rounded build-up to a maximum that occurs well after the start of the signal.

If this signal is due to ballistic phonons, then the shape indicates that more phonons with $\omega \simeq 11$ K are detected than ones with $\omega \simeq 10$ K. It is unlikely that the injected spectrum increases with increasing energy in this range; so it appears that there is some attenuation of the phonons with energies just above ω_c. Such an attenuation can occur with scattering from the low density of ambient thermal phonons via the four-phonon process [21]. Although the thermal phonons are small and each scattering causes only a small change in energy of the large phonon, there can be many scatterings. As the large phonon can increase or decrease its energy at each scattering, the effect of many scatterings is a random walk along the energy axis. As any phonon that drops below ω_c is lost from the high-energy group, this has the effect of decreasing the spectrum just above ω_c.

6. Conclusions

Liquid ^4He has a profound effect on the spectrum of phonons that propagate through it as pressures of less than 19 bar. Above this pressure, phonons propagate ballistically if the temperature is sufficiently low because there are no scattering processes. Below 19 bar the upward dispersion allows strong spontaneous decay processes for phonons with $\omega < \omega_c$; ω_c varies with pressure from 10 K at 0 bar to zero at 19 bar.

We have shown in this study that there can be two propagating groups of phonons. A group with ω above ω_c propagates without interaction if the ambient temperature is sufficiently low. At finite temperatures there is four-phonon process scattering with the thermal phonons which depletes the modes just above ω_c. The other group of phonons contain the decay products from injected phonons with $\omega < \omega_c$. These travel at the ultrasonic velocity. If this group has a high density, then the phonons in it strongly interact via the three-phonon process. This entails energy up-scattering as well as down-

scattering and there will be a dynamic occupation of phonon modes. The higher the phonon density, the more the phonon spectrum will extend in energy. At input energies of about −10 dB or more (reference 0.5 W mm^{-2}) this interacting group completely dominates the occupation of all phonon modes. However, at low powers (about −20 dB or less) the interacting phonons can be ignored above $\omega = 4$ K, and liquid He can be used to study the propagation and interactions of very high-energy phonons.

Acknowledgment

The experimental work was done while the authors were at the University of Nottingham.

References

[1] Cowley R A and Woods A D B 1971 *Can. J. Phys.* **49** 177–200
[2] Landau L D 1941 *J. Phys. Moscow* **5** 71; *JEPT Lett.* **11** 592
[3] Maris H J and Massey W E 1970 *Phys. Rev. Lett.* **25** 220
[4] Khalatnikov I M 1965 *Theory of Superfluidity* (New York: Benjamin)
[5] Mills N G, Sherlock R A and Wyatt A F G 1974 *Phys. Rev. Lett.* **32** 978; 1975 *J. Phys. C: Solid State Phys.* **8** 2575
[6] Jackle J and Kehr K W 1971 *Phys. Rev.* **27** 654
[7] Dynes R C and Narayananurti V 1974 *Phys. Rev. Lett.* **33** 1195
[8] Wyatt A F G, Lockerbie N A and Sherlock R A 1974 *Phys. Rev. Lett.* **33** 1425–8
[9] Stirling W G 1983 *Proc. 75th Conf. Liquid Helium* vol 4 ed. J G M Armitage (Singapore: World Scientific) pp 109–11
[10] Baird M J, Hope F R and Wyatt A F G 1983 *Nature* **304** 325–6
[11] Dietsche W and Kinder H 1976 *J. Low Temp. Phys.* **23** 27
[12] Sherlock R A, Wyatt A F G and Lockerbie N A 1977 *J. Phys. C: Solid State Phys.* **10** 2567–81
[13] Wyatt A F G and Crisp G N 1978 *J. Physique Coll.* **39** C6 244–5
[14] Wyatt A F G, Sherlock R A and Allum D R 1982 *J. Phys. C: Solid State Phys.* **15** 1897–915
[15] Brown M and Wyatt A F G to be published
[16] Bradshaw T W and Wyatt A F G 1983 *J. Phys. C: Solid State Phys.* **16** 651–64
[17] Maris H J 1977 *Rev. Mod. Phys.* **49** 341
[18] Slukin T J and Bowley R M 1974 *J. Phys. C: Solid State Phys.* **7** 1779–85
[19] Nothdurft E E and Luszczynski K 1978 *J. Physique* **39** C6 252–3
[20] Wyatt A F G and Page G J 1978 *J. Phys. C: Solid State Phys.* **11** 4927–44
Sherlock R A, Mills N G and Wyatt A F G 1975 *J. Phys. C: Solid State Phys.* **8** 300–15
[21] Korcynskyj Y and Wyatt A F G 1978 *J. Physique* **39** C6 230–1
[22] Wyatt A F G 1987 *Japan. J. Appl. Phys.* **26** suppl. 26–3, 7–8